# Correlations between energy and mass partition in the damped reaction $^{165}Ho+^{74}Ge$ at $E_{lab}=8.5$ MeV/nucleon

J. Tõke, R. Płaneta,* W. U. Schröder, and J. R. Huizenga
*Departments of Chemistry and Physics and Nuclear Structure Research Laboratory, University of Rochester, Rochester, New York 14627*
(Received 21 January 1991)

Data from a kinematical coincidence experiment on the damped reaction $^{165}Ho+^{74}Ge$ at 8.5 MeV/nucleon have been reanalyzed. Although the new analysis confirms the presence of some correlations between the excitation-energy division and the mass asymmetry, the magnitude of these correlations is found to be significantly smaller than that previously reported. Proton-neutron symmetry of the mechanism of heat generation through nucleon exchange is revealed and a possible acceptor-donor asymmetry of this mechanism is discussed.

## I. INTRODUCTION

Over the many years of experimental and theoretical studies of damped heavy-ion reactions at energies of a few MeV/nucleon above the Coulomb barrier, a picture has emerged, in which the contact or interaction stage of such a reaction is viewed as a rapid succession of many "elementary" processes, the stochastic nucleon exchange of independent nucleons between the two reaction partners. Such a picture, expressed most clearly in the one-body nucleon exchange model [1], finds support in a large body of experimental data on various correlations between experimental observables in damped reactions [2]. Of particular importance for a thorough understanding of the microscopic mechanisms, underlying the dissipative nature of these reactions, are experimental studies of the redistribution of the dissipated energy between the two reaction partners as a function of total-kinetic-energy loss $E_{loss}$. Until recently, most studies of this kind have focused on two-dimensional correlations in the space of observables, e.g., those between the excitation-energy division and $E_{loss}$. Results from several early experiments on such two-dimensional correlations were interpreted as providing indication for a virtually complete thermal equilibrium, attained by the reaction partners already at very early stages of the collision. However, later experiments, employing various experimental techniques [3–10] led to the rather firm establishment of a contrasting view. These studies have ascertained that at the initial stages of the interaction, the excitation energies of the two fragments are nearly equal, when averaged over all fragment mass asymmetries. Thus, for mass-asymmetric systems, a considerable thermal disparity between the two reaction fragments was shown to persist at least for relatively low total-kinetic-energy losses. A clear trend to approach a thermal equilibrium with increasing kinetic-energy loss has also been well established. However, the thermal-equilibrium limit, where the total excitation energy is divided between the fragments in proportion to their masses, seems not be reached even at very large energy losses. The above experimental correlations, integrated over the fragment mass asymmetries, are in qualitative agreement with the predictions of the one-body nucleon exchange model [1]. Occasional difficulties in obtaining a full, quantitative agreement between data and calculations, performed using some systematic estimates for the values of the model parameters, seem not to provide a firm basis for questioning the validity of the nucleon exchange model.

Progress in experimental techniques has provided the opportunity to study more refined, three-dimensional correlations between the experimental observables, with the additional third dimension being the fragment mass asymmetry. Two experiments investigating the correlation between excitation-energy division and fragment mass asymmetry as a function of $E_{loss}$ have been carried out [8–10] using the kinematical coincidence method (KCM). Based on the analysis of data from these two experiments, the presence of strong correlations between excitation-energy division and net mass transfer was reported [8–10] for the full range of $E_{loss}$. Since strong correlations of this kind are difficult to reconcile with the one-body nucleon exchange model [1], alternative models that [11–13] claim to be capable of explaining the reported correlations between mass and energy division have been promoted. Recently, however, a dominantly instrumental origin was demonstrated [14] for the correlations claimed [8] in the case of the $^{165}Ho+^{56}Fe$ reaction. In the present paper, as in previous work [14,15], the term "instrumental correlations" is used for the artificial correlations between experimental observables resulting from intrinsic imperfections of both the instruments and the methods used in an experimental study. It was shown [14] that the $^{165}Ho+^{56}Fe$ data, published [8] for an energy loss of $E_{loss}=125$ MeV, are compatible with the assumption of an excitation-energy division independent of the net mass transfer or mass asymmetry. Most, if not all,of the reported correlations were found to have resulted from the inherent finite-mass resolution of the kinematical coincidence method (KCM), due mostly to particle emission from the two highly excited primary reaction fragments. The previous analysis [14] was limit-

 

ed to data in a single bin of relatively high kinetic-energy losses and was unable to determine unambiguously whether or not physical correlations were actually present at some low level. Such ambiguities result from the fact that the instrumental correlations coincide in both character and approximate magnitude with the ones observed for the $^{165}$Ho+$^{56}$Fe reaction. In view of substantial uncertainties in the fragment mass determination generated by evaporation processes, it was difficult [14] to interpret any residual difference between observed and estimated instrumental correlations in terms of physical correlations.

Subsequently, an alternative method of interpreting the data obtained from kinematical coincidence experiments in terms of excitation-energy division has been proposed [15]. This latter analysis procedure has been shown to be far less sensitive to the finite-resolution effects than more conventional methods. A much higher confidence in this new analysis procedure has provided the motivation for a reanalysis of the data from the experiment of Refs. [9] and [10]. The aim of the reanalysis reported in the present paper is to provide a reasonably accurate, quantitative determination of the magnitude of the physical correlations between excitation-energy division and net mass transfer as a function of $E_{\rm loss}$. Such a reanalysis appears to be called for also in view of the fact that the two published accounts [9,10] of this experiment, differ in their assessment of the quality of the experimental setup and, hence, the quoted magnitude of the instrumental correlations. Furthermore, the results presented in these papers were contaminated by significant instrumental artifacts and did not establish the actual magnitude of correlations which are of fundamental importance for the understanding of the reaction mechanism.

In Sec. II, experimental procedures [9,10] are reviewed, with particular emphasis on instrumental correlations resulting from finite-resolution effects, and the new analysis procedure is outlined. Section III presents and discusses the results of this reanalysis. The findings are summarized in Sec. IV.

## II. EXPERIMENTAL PROCEDURE AND ANALYSIS METHODS

The aim of the original experiment [9,10] was to identify the exit channels of the damped reaction $^{165}$Ho+$^{74}$Ge at $E/A=8.5$ MeV according to total-kinetic-energy loss $E_{\rm loss}$, primary (preevaporation) fragment masses, as well as secondary (postevaporation) masses and the atomic numbers $Z$ of projectilelike fragments (PLF). Details of the experimental procedure are described in Refs. [9] and [10]. For the PLF, the experiment measured directly the angle $\theta_{\rm PLF}$, the energy $E$, the energy $\Delta E$ lost in a transmission detector, and the time of flight (TOF) between the transmission ($\Delta E$) and stop ($E$) detectors. In addition, the recoil angle $\theta_{\rm TLF}$ of the targetlike fragment (TLF) was measured in coincidence with its PLF reaction partner.

These raw data were converted event by event into the quantities related to the reaction exit channel, in an off-line analysis. Based on the velocity vector of a PLF and the recoil angle of the associated TLF, the total-kinetic-energy loss $E_{\rm loss}$ and the primary masses of PLF and TLF were calculated, using proper kinematical formulas. The secondary mass of the PLF was calculated from its energy and time of flight, and the respective atomic number of the PLF was determined based on the $\Delta E$-$E$ correlation. Next, in an iterative procedure involving the statistical evaporation code PACE [16], the excitation energy of the PLF and its preevaporation atomic number was determined. The latter atomic number combined with the primary mass of the PLF allowed one to determine the $Q_{gg}$ value of the reaction and, consequently, to deduce the total excitation energy $E^*_{\rm tot}$. The above procedure of converting the raw data into the quantities of interest was followed in both the original [9,10] and the present analyses. However, the two analysis procedures differ significantly in the way in which correlations between primary mass asymmetry and excitation-energy division are evaluated. As demonstrated previously [14,15], the procedure of relating calculated excitation-energy division to calculated primary mass followed in the earlier analyses [8–10] introduces significant instrumental correlations between the deduced values for these observables. Such spurious correlations result from the systematic, mass-dependent, deviation of the apparent "primary" mass, $A_{\rm calc}$, calculated event by event from kinematical reconstruction formulas, from the actual "true" primary mass $A_{\rm prim}$. It can be shown [14,15] that for Gaussian-distributed primary masses and a Gaussian mass resolution function, the relation between $A_{\rm calc}$ and the average true primary mass $\langle A_{\rm prim}\rangle$ it represents, is given by

$$\langle A_{\rm prim}\rangle = A_{\rm calc} + (A_{\rm calc} - A_0)\frac{\sigma^2_{\rm res}}{\sigma^2_A + \sigma^2_{\rm res}}\ , \qquad (1)$$

where $A_0$ is the actual centroid of the primary mass distribution, and $\sigma^2_{\rm res}$ and $\sigma^2_A$ are the variances of the mass resolution function and the primary mass distribution, respectively. Systematical errors in assigning values to the (average) primary masses, introduced by neglecting the second term on the right-hand side of Eq. (1), lead to systematical errors in the deduced average excitation energies depending on the primary mass. As seen from this equation, the magnitude of the resulting instrumental correlations depends critically on the mass resolution. Therefore, in order to extract the magnitude of the actual (physical) correlations between excitation-energy division and the primary PLF mass, one must know this resolution precisely.

Two factors influence the accuracy with which the primary mass is determined in an experiment. One factor depends on the quality of the experimental apparatus, e.g., the angular resolution achieved with the two (PLF and TLF) detectors, the resolution of the TOF measurement, the size of the beam spot on the target, the angular straggling of the TLF in the target, etc. The role of this factor can be controlled to a certain degree. The second factor, inherent in the KCM, results from the random alterations of the fragment velocity vectors by the recoils imparted on the fragments by the particles evaporated in

flight. The experiment [9,10] under discussion did not provide for adequate direct cross-checks that could have been used to determine this critical intrinsic mass resolution experimentally. Hence, the earlier analysis method of sorting data from this experiment into bins in calculated primary mass does not provide an unambiguous quantitative answer regarding the correlations in question.

In contrast, the present analysis follows the suggestion of Ref. [15] and sorts data into bins in secondary, postevaporation mass. The secondary mass is determined with much better resolution than the primary mass. Moreover, at all kinetic-energy losses, one actually resolves the lines corresponding to the various masses, and hence one can actually measure the respective resolution. By sorting the data into bins in secondary mass, one effectively averages over the apparent primary masses $A_{\rm calc}$. Hence, the instrumental correlations between excitation energy and mass, arising from the finite resolution in primary mass, average out. This method of binning in secondary mass introduces instrumental correlations associated with finite resolution in secondary mass. However, due to the much better resolution in secondary mass, these latter correlations are much smaller in magnitude and easier to account for than those associated with the primary mass. From the present analysis of the raw experimental data, it was found that the variance of the secondary-mass resolution function is approximately $\sigma^2_{\rm res}=0.29$, i.e., equal to the variance of a Gaussian distribution with FWHM$=1.27$. In contrast to the good resolution in secondary mass, the measured variance of the elastic line in the primary mass distribution is already 0.7. Furthermore, Monte Carlo simulations employing the actual non-Gaussian shape of the elastic line yield values of 1.0 and 5.0 for this variance for energy losses of 40 and 170 MeV, respectively. The above values are significantly higher than one would obtain based on the original evaluations [17] postulating a Gaussian resolution function (0.5 and 4.3 from 40 and 170 MeV, respectively). It should be stressed that the finite-resolution effects under discussion scale quite accurately with the variance of the resolution function and not with its FWHM. As the actual resolution functions are non-Gaussian, their FWHM do not provide a proper measure of the quality of the experimental setup. As an example, the resolution function in secondary mass has a width of only FWHM$=0.6$, yet it generates finite-resolution effects equal to those generated by a Gaussian with FWHM twice as large. In the Monte Carlo simulations performed in the present work and discussed in the next section, a secondary-mass resolution function was employed which approximated the actual resolution function.

## III. EXPERIMENTAL RESULTS

Figure 1 shows the "raw" correlations between the secondary PLF mass $A_{\rm sec}$ and the excitation-energy division, represented by the fraction $\langle E^*_{\rm PLF}/E^*_{\rm tot}\rangle$ of the total excitation energy $E^*_{\rm tot}$ deposited in the primary PLF. The relatively weak correlations seen in this figure are very different in character from the strong dependencies of the above fraction on the reconstructed primary mass $A_{\rm calc}$, reproduced in Fig. 2. In the earlier analysis [10] the latter type of dependences have been interpreted in terms of strong correlations between excitation-energy division and primary fragment mass asymmetry. It is important to emphasize here that the results shown in Figs. 1 and 2 are generated from the same set of quantities, deduced from an event-by-event data analysis. Hence, they

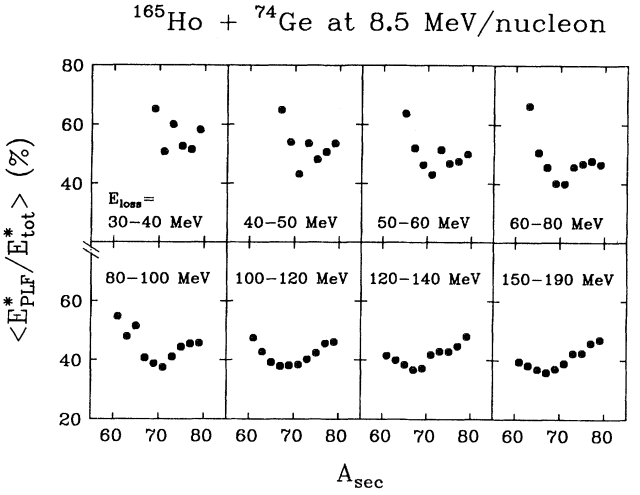


FIG. 1. Correlations between the excitation-energy division and the secondary (postevaporation) mass of the PLF seen in a straightforward analysis which does not include finite-resolution corrections.

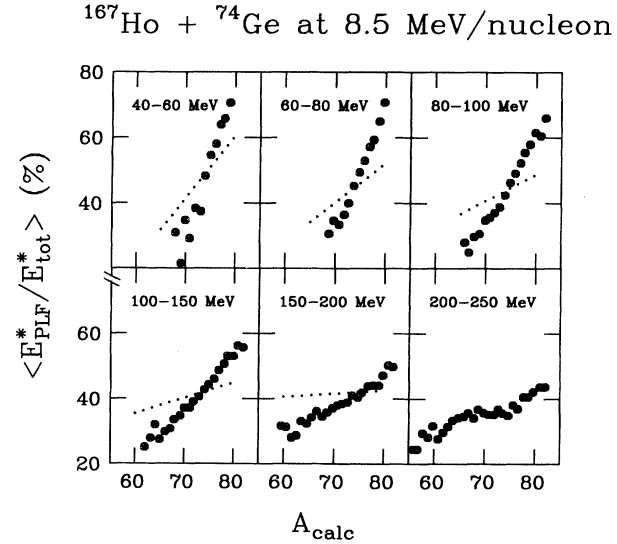


FIG. 2. Correlations between the excitation-energy division and the primary (preevaporation) mass of the PLF seen in a straightforward analysis which does not include finite-resolution corrections [9,10] (solid dots). Dotted lines show the physical correlations assumed in the respective Monte Carlo simulations which are required in order to fit the observed correlations (see Fig. 4).

must be reproduced simultaneously by any sound simulation calculation. The correlations in Figs. 1 and 2, however, cannot be reconciled with each other through Monte Carlo simulations of particle evaporation from the PLF alone. Only when account is taken of the critical finite-resolution effects [14] for both fragments can these correlations be understood consistently.

In Fig. 3, correlations between the average evaporated ("missing") mass, $\langle A_{\rm calc} - A_{\rm sec} \rangle$, and the secondary mass $A_{\rm sec}$ are displayed for the indicated bins in total-kinetic-energy loss. These are results of a straightforward analysis in which no corrections are made for the finite-resolution effects. The quasiparabolical patterns seen at small energy losses are understood to arise from correlations between the (finite-resolution) errors of the calculated quantities, mass and $E_{\rm loss}$, which are both mostly due to the finite resolution in the emission angle of the TLF. In a straightforward analysis, these correlations prevent a proper averaging over the apparent mass $A_{\rm calc}$ within a given $E_{\rm loss}$ bin. This is due to the fact that the events are sorted into wrong $E_{\rm loss}$ bins, in a systematic fashion depending on the error in $A_{\rm calc}$. In order to avoid such a mass-correlated misbinning of events, in the present analysis a procedure was adopted in which $E_{\rm loss}$ was calculated iteratively from the measured secondary mass and an assumed evaporated mass. Results of these calculations are shown in Fig. 4, where the missing mass is plotted versus the measured secondary mass as a function of the iteratively calculated $E_{\rm loss}$. The representation used in Fig. 4 is well suited for an analysis of the correlations between the physical quantities, as it does not involve any Monte Carlo simulations of the particle evaporation processes. The results of the Monte Carlo simulations for the correlations between evaporated and secondary mass are shown in Fig. 5, for four selected

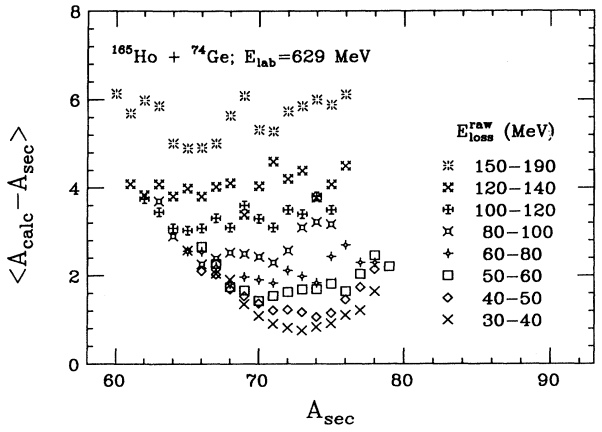


FIG. 3. Correlations between the evaporated mass and the secondary mass of the PLF seen in a straightforward analysis which does note include finite-resolution corrections. The quasiparabolical character of these correlations at small kinetic energy losses results from the correlations between the finite-resolution errors of the calculated $E_{\rm loss}$ and calculated primary mass of the PLF.

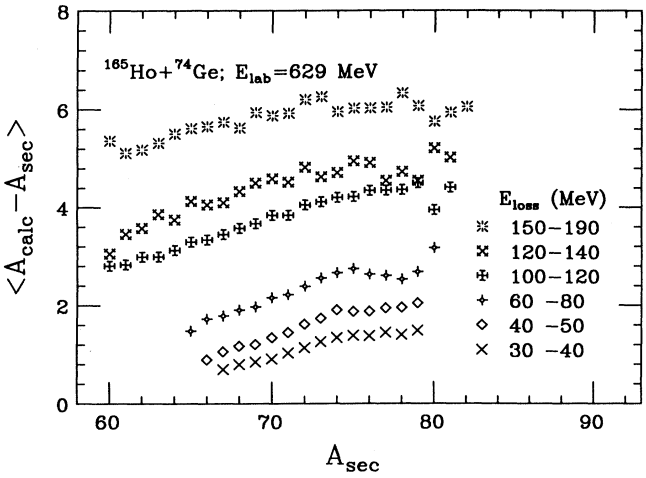


FIG. 4. Correlations between the evaporated mass and the secondary mass of the PLF as a function of corrected $E_{\rm loss}$, calculated in an iterative fashion (see text).

$E_{\rm loss}$ bins. Open diamonds in this figure represent calculations with "best-choice" assumptions regarding the physical dependence of excitation-energy division on primary mass. These best-choice assumptions are quite accurately approximated by a linear function in $A_{\rm prim}$:

$$E^*_{\rm PLF} = C + R E^*_{\rm tot}(A_{\rm prim} - A_0) , \quad (2)$$

relating the excitation energy $E^*_{\rm PLF}$ of the primary PLF to the total excitation energy $E^*_{\rm tot}$. In Eq. (2), $C$ and $R$ are $E_{\rm loss}$-dependent parameters. These assumptions are summarized in Table I in terms of parameters $C$ and $R$.

TABLE I. Results of the Monte Carlo simulations for the observed correlations between the secondary mass and the evaporated mass. Parameters $C$ and $R$ describe the assumed correlations between the excitation-energy division and the primary mass, necessary to obtain fits to the experimental data shown in Fig. 5. The last column shows the asymmetry $\eta$ between the excitation energies generated in the acceptor and donor fragments in a single nucleon exchange process, as estimated from Eq. (3). The uncertainties in the quantity $R$, expressing the magnitude of the correlations between the net mass transfer and the excitation-energy division, are estimated to be approximately 30%, except for the last $E_{\rm loss}$ bin, where the error is estimated to be +50%, −100%. These estimates are based on the sensitivity of the quality of the obtained fits, such as those presented in Fig. 5, to the assumed value of $R$.

| $E_{\rm loss}$ (MeV) | $E^*_{\rm PLF} = C + R E^*_{\rm tot}(A_{\rm prim} - A_0)$ $C/E^*_{\rm tot}$ (MeV$^{-1}$) | $R$ | $\eta$ |
|---|---|---|---|
| 36 | 0.48 | 0.030 | 0.35 |
| 44 | 0.50 | 0.025 | 0.33 |
| 65 | 0.45 | 0.012 | 0.30 |
| 110 | 0.43 | 0.006 | 0.35 |
| 130 | 0.42 | 0.005 | 0.90 |
| 170 | 0.42 | 0.001 | −0.53 |

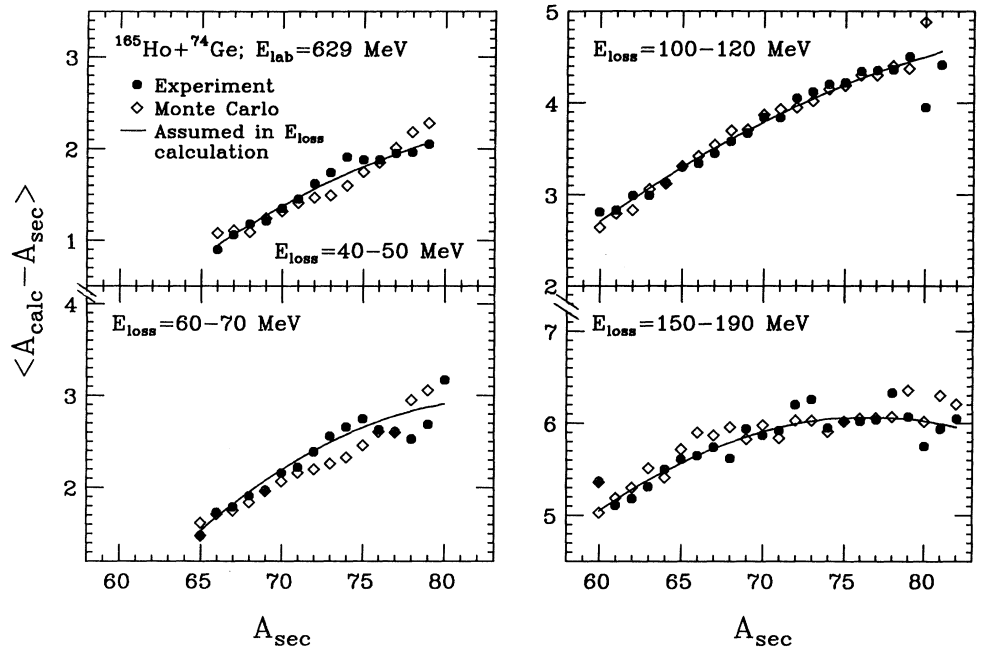


FIG. 5. Analysis of the correlations between the evaporated mass and the secondary mass for selected bins in $E_{loss}$. Solid dots are the experimental results as shown in Fig. 4, and the diamonds are the results of the Monte Carlo simulations with best-choice assumptions (see Table I and also Fig. 2) for the physical correlations between the excitation-energy division and the net mass transfer. Solid lines show the final assumption made on the average evaporated mass in the iterative procedure of calculating $E_{loss}$.

The physical correlations between net mass transfer and excitation-energy division deduced, in the present analysis, are significantly weaker than those claimed in Refs. [9] and [10], especially at the higher energy losses. The disappearance of these correlations ($R \rightarrow 0$) for the $^{165}$Ho+$^{74}$Ge reaction at the high energy losses is in agreement with the findings of an earlier analysis carried out [14] for the $^{165}$Ho+$^{56}$Fe reaction.

In Fig. 6, the strengths of the correlations are illustrated in terms of the slope parameter $R$. Two sets of points are displayed in Fig. 6 to demonstrate the importance of the finite-resolution effects. The solid squares represent the trends observed in the experimental data of Fig. 2 and, hence, obtained by neglecting [9,10] the resolution effects. In contrast, the solid dots result from the present analysis taking quantitative account of these finite-resolution effects. It is noticed that at $E_{loss}$ values of 50 and 170 MeV, the values of the quantity $R$ obtained in the two analyses differ by factors of 2.4 to 8.0.

It appears plausible that correlations between excitation-energy division and net mass transfer arise from the inherent differences between the excitation energies generated in the acceptor and donor fragments in each of the successive nucleon exchange processes. It is then interesting to explore the dependence of this acceptor-donor asymmetry on impact parameter or total kinetic-energy loss. For example, in a nucleon exchange model [1], where the deposited energy depends on the velocity mismatch between the fragments, one expects a gradual decrease of this asymmetry with increasing energy loss. One can also speculate that the time evolution of the window between the fragments could lead to a similar dependence on $E_{loss}$. The following formula has been derived (see Appendix), to relate the measured quantities $R$ and $\sigma_A^2$ to the asymmetry between the excitation energies generated in the acceptor and donor fragments in the

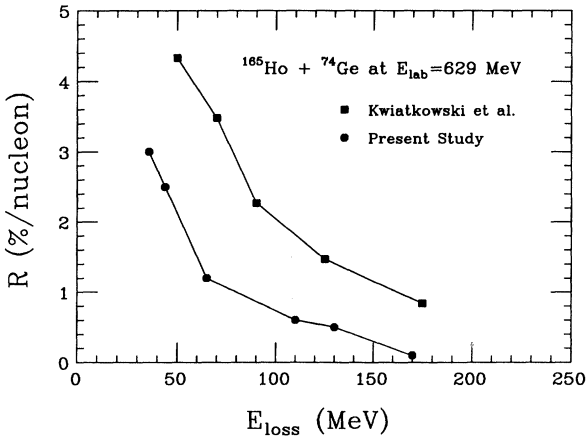


FIG. 6. Comparison of the strengths of the correlations between the excitation-energy division and the net mass transfer in terms of the slope parameter $R$ [see Eq. (2)] deduced in the straightforward analysis of Refs. [9] and [10] (solid boxes) and in the present analysis (solid dots).

process of one nucleon exchange (transfer):

$$\eta=\frac{e_a-e_d}{e_a+e_d}=\frac{d(E^*_{\rm tot}R\sigma^2_A)}{dE_{\rm loss}}\Big/\frac{d\langle E^*_{\rm PLF}\rangle}{dE_{\rm loss}}\ . \tag{3}$$

In Eq. (3), $e_a$ and $e_d$ are the excitation energies generated in the acceptor and donor fragment, respectively. Note that the quantity $\eta$ defined by Eq. (3) has a character fundamentally different from that of the quantities such as $\sigma^2_A$, $E_{\rm loss}$ and parameters $C$ and $R$ in Eq. (2). While the latter quantities describe a cumulative effect, integrated over the whole interaction period, the asymmetry defined in Eq. (3) is a differential quantity and describes the effects taking place at a particular stage of the collision, after a given amount of kinetic energy has been dissipated. Estimates of the acceptor-donor asymmetry based on Eq. (3) are presented in the last column of Table I. These asymmetries are remarkably constant, for most of the energy-loss range considered. The large fluctuations seen at $E_{\rm loss}=130$ and 170 MeV can easily be attributed to the uncertainties in the best-choice values of the parameters $R$ and $C$ [see Eq. (2)] obtained in a series of Monte Carlo simulations. As seen from Table I, a moderate acceptor-donor asymmetry of the heat-generation mechanism is present at any stage of the damped collision. Somewhat unexpected or surprising is the fact that this asymmetry stays relatively constant throughout the history of the dinuclear system. Note that the quantity $R$ at the same time decreases almost to zero as $E_{\rm loss}$ increases. This expresses the simple fact that from the many nucleon exchanges contributing to $E^*_{\rm tot}$, only a few (net transfer) are responsible for the cumulative effect in $R$. The above fact supports also the usefulness of the differential quantity such as $\eta$ to characterize an individual exchange process. Here, a word of caution is due regarding Eq. (3). The compactness and simplicity of this formula results from a number of assumptions made in derivation. It remains to be established by full stochastic nucleon exchange model calculations how critical these simplifying assumptions are for the extracted values of the acceptor-donor asymmetry $\eta$.

Figure 7 shows the correlations between the secondary mass and the evaporated mass for the various measured atomic numbers $Z$ of the PLF indicated by different symbols. The qualitative difference between the correlations displayed in Figs. 7(a) and 7(b) illustrates again the importance of finite-resolution corrections for the analysis. Figure 7(a), where no corrections were made for the secondary-mass resolution, indicates a clear dependence of the evaporated mass of the species of transferred nucleon. Monte Carlo simulations, however, show that this type of proton-neutron asymmetry is completely of instrumental origin, due to the finite resolution in secondary mass. Figure 7(b) includes the finite-resolution corrections, and hence shows the pure physical correlations. In this figure, correlation patterns for different $Z$ values define a common curve, indicating an independence of the heat-generation mechanism of the type of nucleon transferred, a proton-neutron symmetry of this mechanism.

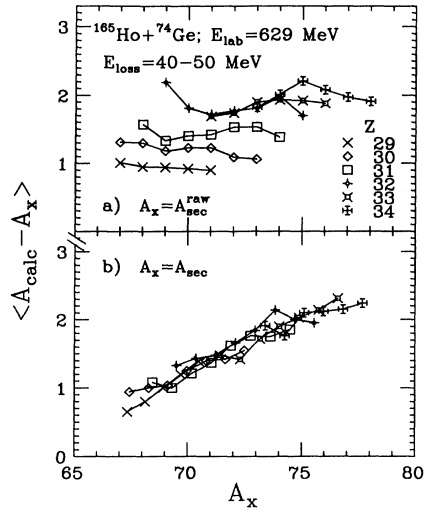


FIG. 7. Correlations between the evaporated mass and the secondary mass of the PLF gated with the atomic number of PLF, seen without (a) and with (b) finite-resolution corrections for the secondary mass.

## IV. CONCLUSIONS

The present study confirms the existence of correlations between excitation-energy division and net mass transfer in the damped reaction $^{165}$Ho+$^{74}$Ge at 8.5 MeV/nucleon. The magnitude of these correlations is, however, significantly smaller than reported earlier [9,10]. While at small kinetic-energy losses, the results from the earlier [9,10] and the present analyses differ by a factor of 2; at high energy losses the difference is by a factor of approximately 8. The source of these discrepancies is the finite-resolution effects, which play a critical role in the earlier analysis carried out according to the straightforward method.

The above correlations can be attributed to the asymmetry between the excitation energies generated in acceptor and donor fragments by each individual nucleon exchange process. Although in the multinucleon exchange process PLF and TLF assume the roles of donor and acceptor alternatively, some correlations between excitation-energy and mass division survive. Estimates based on Eq. (3) suggest that a moderate acceptor-donor asymmetry is present throughout the damped interaction, such that the acceptor fragment receives on the average approximately 65% of the total kinetic energy dissipated in each individual exchange, whereas the donor receives only 35% of this energy. The independence of this asymmetry on $E_{\rm loss}$ or interaction time is somewhat surprising, since in the course of the reaction the dinuclear system is expected to undergo significant changes, e.g., as far as relative velocity, window geometry, and interaction barrier are concerned. Such an independence suggests that the above properties of the dinuclear system do not play a major role in generating the acceptor-donor asymmetry. The observed proton-neutron symmetry of the heat-generation mechanism provides further support for such

a conclusion. The fact that both the net proton and the neutron transfers generate equal patterns in the excitation-energy division, even at low energy losses, indicates that the forces encountered by the nucleons traversing the "windows" between the interacting fragments are too small to influence these patterns.

At any rate, if confirmed by more detailed model comparisons, the persistence and constance of the above acceptor-donor asymmetry throughout the reaction history presents a challenge to the current understanding of the damped-reaction mechanism.

## ACKNOWLEDGMENTS

This work was supported by the United States Department of Energy under Grant No. DE-FG02-88ER40414. The authors wish to express their gratitude to the Indiana University Nuclear Chemistry group and their collaborators for their cooperation and for giving access to their raw data.

## APPENDIX

In the following, Eq. (3) is derived for the elementary asymmetry $\eta$ between the excitation energies generated in the acceptor and donor fragments in an individual nucleon exchange. The asymmetry $\eta$ is a differential quantity referring to a particular stage of the collision, after a certain amount of macroscopic kinetic energy has been dissipated, or a certain interaction time has elapsed. The differential character of this quantity makes a strong reference to the one-body exchange picture of the damped collision as an evolutionary process, consisting of a rapid succession of many small changes. Note that the most commonly used observables in analyses of damped collisions such as, e.g., $E_{\rm loss}$, $\sigma_A^2$, $\sigma_Z^2$, $A$ and $Z$ drift, as well as the slope parameter $R$ introduced in Eq. (2), are integral variables. They reflect various cumulative effects of the heavy-ion interaction, integrated over the whole duration of the interaction. The following derivation is based on the fact that the correlations between excitation-energy division and primary mass $A_{\rm prim}$ are quite well approximated by the linear formula of Eq. (2). Additionally, it is assumed that collisions leading to different values of $E_{\rm loss}$ evolve along a common path in the space of the relevant collision parameters such as $\sigma_A^2$, $R$, and $C$ [Eq. (2)], $E^*_{\rm PLF}$ and $E^*_{\rm tot}$. The latter assumption is an approximation, as different values of $E_{\rm loss}$ are expected to involve different partial waves in the entrance channel and, therefore, different system trajectories.

Consider the system of interacting fragments at two close instances in time $t_1$ and $t_2$ when the respective values of kinetic-energy loss are $E_{\rm loss}$ (1) and $E_{\rm loss}$ (2), and variances of the PLF mass distribution are $\sigma_A^2$ (1) and $\sigma_A^2$ (2). Furthermore, for the sake of simplicity, it is assumed that the centroid of this mass distribution remains at a constant value of $A_0$. The number of nucleon exchanges taking place between these two instances can be approximated as $N_{\rm exch}=\sigma_A^2(2)-\sigma_A^2(1)$. This number $N_{\rm exch}$ is the sum of the numbers of exchanges where the PLF is the donor ($N_d$) and those where it is acceptor ($N_a$):

$$N_{\rm exch}=N_a+N_d=\sigma_A^2(2)-\sigma_A^2(1)\ . \tag{A1}$$

A given bin in PLF mass $A_{\rm prim}$ at $E_{\rm loss}$ (2) is fed by various mass bins at $t_1$, i.e., $E_{\rm loss}$ (1), as a result of a series of nucleon exchanges. The average mass $\langle A_{\rm prim}(1)\rangle$ at $t_1$, contributing to the bin at $A_{\rm prim}$ at $t_2$ is equal to

$$\langle A_{\rm prim}(1)\rangle = A_{\rm prim}-(A_{\rm prim}-A_0) \times[\sigma_A^2(2)-\sigma_A^2(1)]/\sigma_A^2(2)\ . \tag{A2}$$

Note the similarity of Eqs. (1) and (A2), both of which describe the broadening of Gaussian distributions as a result of stochastic processes. The second term on the right-hand side of Eq. (A2) represents an average net transfer of nucleons to or from the PLF, for $A_{\rm prim}>A_0$ and $A_{\rm prim}<A_0$, respectively. The number $N_{\rm tr}$ of transferred nucleons can be expressed through the numbers $N_d$ and $N_a$ introduced above, by

$$N_{\rm tr}=N_a-N_d=(A_{\rm prim}-A_0)[\sigma_A^2(2)-\sigma_A^2(1)]/\sigma_A^2(2)\ . \tag{A3}$$

Equations (A1) and (A3) can be solved for $N_a$ and $N_d$:

$$N_a=\tfrac{1}{2}[\sigma_A^2(2)-\sigma_A^2(1)]+\tfrac{1}{2}(A_{\rm prim}-A_0)\frac{\sigma_A^2(2)-\sigma_A^2(1)}{\sigma_A^2(2)}\ ,$$

$$N_d=\tfrac{1}{2}[\sigma_A^2(2)-\sigma_A^2(1)]-\tfrac{1}{2}(A_{\rm prim}-A_0)\frac{\sigma_A^2(2)-\sigma_A^2(1)}{\sigma_A^2(2)}\ . \tag{A4}$$

The average excitation energy of the PLF for the mass bin at $A_{\rm prim}$ at $t_2$ is given by Eq. (2) directly. On the other hand, it can be related to the average PLF excitation energy for mass bin centered at $A_{\rm prim}$ (1) [see Eq. (A2)] at $t_1$:

$$\begin{aligned}E^*_{\rm PLF}(2)&=C(2)+R(2)E^*_{\rm tot}(2)(A_{\rm prim}-A_0)\\ &=C(1)+R(1)E^*_{\rm tot}(1)[\langle A_{\rm prim}(1)\rangle-A_0]\\ &\quad+N_a e_a+N_d e_d\ ,\end{aligned} \tag{A5}$$

where $e_a$ and $e_d$ denote the excitation energies acquired by the acceptor and donor fragment, respectively, in a single nucleon exchange. The two last terms on the right-hand side of Eq. (A5) describe the average excitation acquired by the PLF as a result of accepting and donating nucleons.

By substituting Eqs. (A1) and (A4) into Eq. (A5) and requiring that the latter be fulfilled at any value of $A_{\rm prim}$, one obtains two equations relating $e_a$ and $e_d$:

$$e_a - e_d = \frac{2[R(2)E^*_{\rm tot}(2)\sigma^2_A(2) - R(1)E^*_{\rm tot}(1)\sigma^2_A(1)]}{[\sigma^2_A(2) - \sigma^2_A(1)]}, \qquad (A6)$$

$$e_a + e_d = 2[C(2) - C(1)]/[\sigma^2_A(2) - \sigma^2_A(1)] .$$

Equations (A6) relate the acceptor-donor asymmetry of the heat-generation mechanism to the experimental observables $\sigma^2_A$, $E^*_{\rm tot}$, $C$, and $R$. They can be cast into a compact differential form:

$$\eta = \frac{e_a - e_d}{e_a + e_d} = \frac{d(E^*_{\rm tot} R \sigma^2_A)}{dE_{\rm loss}} \Big/ \frac{d\langle E^*_{\rm PLF}\rangle}{dE_{\rm loss}} , \qquad (A7)$$

where $R$ is the slope parameter of Eq. (2), and the average excitation energy of the PLF, $\langle E^*_{\rm PLF}\rangle$, has been substituted for the parameter $C$ of Eq. (2).

---

*On leave from Jagellonian University, Cracow, Poland.


[1] J. Randrup, Nucl. Phys. **A307**, 319 (1978); **A327**, 490 (1979); **A383**, 468 (1981).

[2] W. U. Schröder and J. R. Huizenga, in *Treatise on Heavy-Ion Science,* edited by D. A. Bromley (Plenum, New York, 1984), Vol. 2, and references therein.

[3] T. C. Awes, R. L. Ferguson, R. Novotny, F. E. Obenshain, F. Plasil, S. Pontoppidan, V. Rauch, G. R. Young, and H. Sann, Phys. Rev. Lett. **52**, 251 (1984).

[4] R. Vandenbosch, A. Lazzarini, D. Leach, D. -K. Lock, A. Ray, and A. Seamster, Phys. Rev. Lett. **52**, 1964 (1984).

[5] H. Sohlbach, H. Freiesleben, P. Braun-Munziger, W. F. W. Schneider, D. Schüll, B. Kohlmeyer, M. Marinescu, and F. Pühlhofer, Phys. Lett. **153B**, 386 (1985); H. Sohlbach, H. Freiesleben, W. F. W. Schneider, D. Schüll, P. Braun-Munziger, B. Kohlmeyer, M. Marinescu, and F. Pühlhofer, Nucl. Phys. **A467**, 349 (1987); H. Sohlbach, H. Freiesleben, W. F. W. Schneider, D. Schüll, B. Kohlmeyer, M. Marinescu, and F. Pühlhofer, Z. Phys. A **328**, 205 (1987).

[6] L. G. Sobotka, G. J. Wozniak, R. J. McDonald, M. A. McMahan, R. J. Charity, L. G. Moretto, Z. H. Liu, F. S. Stephens, R. M. Diamond, and M. A. Deleplanque, Phys. Lett. **175B**, 27 (1986).

[7] J. A. Wile, W. U. Schröder, J. R. Huizenga, and D. Hilscher, Phys. Rev. C **35**, 1608 (1987).

[8] D. R. Benton, H. Breuer, F. Khazaie, K. Kwiatkowski, V. E. Viola, A. C. Mignerey, and A. P. Weston-Dawkes, Phys. Rev. C **38**, 1207 (1988); Phys. Lett. **185B**, 326 (1987).

[9] R. Płaneta, K. Kwiatkowski, S. H. Zhou, V. E. Viola, H. Breuer, M. A. McMahan, J. Randrup, and A. C. Mignerey, Phys. Rev. C **39**, 1197 (1989).

[10] K. Kwiatkowski, R. Płaneta, S. H. Zhou, V. E. Viola, H. Breuer, M. A. McMahan, and A. C. Mignerey, Phys. Rev. C **41**, 958 (1990).

[11] A. Grossman and U. Brosa, Nucl. Phys. **A481**, 340 (1988).

[12] J. Wilczynski and H. W. Wilschut, Phys. Rev. C **39**, 2475 (1989).

[13] J. Wilczynski and K. Siwek-Wilczynska, Phys. Rev. C **41**, R1917 (1990).

[14] J. Tōke, W. U. Schröder, and J. R. Huizenga, Phys. Rev. C **40**, R1577 (1989).

[15] J. Tōke, W. U. Schröder, and J. R. Huizenga, Nucl. Instrum. Methods **A288**, 406 (1990).

[16] A. Gavron, Phys. Rev. C **21**, 230 (1980).

[17] R. Płaneta, K. Kwiatkowski, S. H. Zhou, V. E. Viola, H. Breuer, M. A. McMahan, W. Kehoe, and A. C. Mignerey, Phys. Rev. C **39**, 942 (1989).